




Synergistic antioxidant activity and anticancer effect of green tea catechin stabilized on nanoscale cyclodextrin-based metal–organic frameworks

Fei Ke^{1,*} , Mengran Zhang¹, Nianqiao Qin¹, Gege Zhao¹, Jun Chu², and Xiaochun Wan^{1,*}

¹ State Key Laboratory of Tea Plant Biology and Utilization and Department of Applied Chemistry, Anhui Agricultural University, Hefei 230036, People's Republic of China

² Key Laboratory of Xin'an Medicine, Ministry of Education, Anhui University of Traditional Chinese Medicine, Hefei 230038, Anhui, People's Republic of China

Received: 10 March 2019

Accepted: 5 April 2019

Published online:

11 April 2019

© Springer Science+Business Media, LLC, part of Springer Nature 2019

ABSTRACT

Green tea catechins have received significant attention due to their potent antioxidant activity as well as diverse biological properties. Stabilizing and protecting catechins from degradation is very important but challenging. In this work, a nanosized edible γ -cyclodextrin-based metal–organic framework (CD-MOF) was designed and fabricated by a facile vapor diffusion route and applied for the encapsulation of a model green tea catechin, (-)-epigallocatechin gallate (EGCG) for the first time. Downsizing CD-MOF to the nanoscale is a suitable method to tackle down new applications. Significantly, the antioxidant activity results show that the CD-MOF-EGCG can remarkably enhance the antioxidant activity in alkaline solutions, as compared to that of free EGCG. Furthermore, the prepared CD-MOF-EGCG showed strong cancer cell growth inhibitory effects on C6 cells as confirmed by the cell viability assay. This work demonstrates that such safe and nontoxic nanoscale CD-MOF-based porous materials hold great promise for applications in the field of stabilization of catechins for biomedical applications.

Introduction

Tea has recently attracted significant research interest for its health benefits due to the leaves of tea contain large amounts of catechins [1]. Catechins are natural antioxidants that belong to the polyphenolic flavonoids [2]. Green tea (*Camellia sinensis*) is rich in

catechins, which are present at around 30% of the dry leaf weight [3]. The main catechin polyphenols known to exhibit biological activity are (-)-epicatechin (EC), (+)-catechin (C), (-)-epicatechin gallate (ECG), (-)-gallocatechin gallate (GCG), (-)-epigallocatechin (EGC), and (-)-epigallocatechin gallate (EGCG). The most abundant one in green tea, EGCG

Address correspondence to E-mail: kefei@ahau.edu.cn; xcwan@ahau.edu.cn

possesses the greatest antioxidant activity and is used for cancer therapy because of its high radical-scavenging ability [4, 5]. However, catechins are well known for their chemically unstable in neutral and alkaline aqueous solutions, undergoing oxidation to a semiquinone radical intermediate and formation of quinone oxidized products [6]. Hence, developing suitable methods to stabilize catechins is highly desired. Over the years, several technologies have been explored to protect catechins from degradation and enhance the antioxidant activity. The encapsulation-based method is the most widely used for this purpose in the food industry, such as encapsulation of catechins in chitosan nanoparticles [7], starch nanoparticles [8], edible microhydrogels [9], and β -cyclodextrin [10]. However, there is still more room for the development unfulfilled potentials for improving the stability of catechins.

Metal–organic frameworks (MOFs) are an emergent class of porous materials in which metal ions link organic struts [11, 12]. MOFs have become one of the most intriguing areas, not only for their structural and functional tunability but also for numerous attractive applications, including catalysis [13–18], drug delivery [19–21], gas storage and separation [22], sensing [23], and adsorption [24, 25]. For biomedicine applications, MOFs with large surface areas can be designed and the shape and size of their pores can be controlled to facilitate the adsorption of specific guest molecules [26]. However, most of the reported MOFs based on non-food-grade organic linkers and transition metals are considered to be unacceptable for food, biological, and healthcare applications [27]. In this regard, the development of biocompatible MOFs for healthcare applications is of great importance.

On the other hand, edible γ -cyclodextrin-based MOFs (CD-MOFs) are believed to hold great potential to overcome this problem. CD-MOFs can be easily constructed in the laboratory from food-grade precursors γ -cyclodextrin (γ -CD), and alkali metal salts [28]. They have body-centered cubic structures and large spherical pores of 1.7 nm in diameter accessible through small windows of 0.78 nm [29]. To date, there have been a few pioneering works on CD-MOFs as promising carriers for drug delivery applications [30–32]. Very recently, Moussa and co-workers reported on the application of CD-MOFs to store and stabilize curcumin [33]. However, the utilization of CD-MOFs as carriers for encapsulation of catechins

has no prior report. Moreover, most of the reported CD-MOFs are microcrystals [27–29, 31–33]. The size of porous carriers is critical for their applications. Nanocarriers, due to their smaller particle size, can indeed improve the biomedicine performances. Therefore, it remains an important challenge to develop a facile method to produce small nanocrystals of CD-MOFs for encapsulation of catechins.

Herein, we report a facile method for the synthesis of a novel nanometer-sized CD-MOF, which shows promising application potential in the encapsulation of EGCG for antioxidant activity and tumor therapy. The monodisperse CD-MOF nanocrystals have been successfully synthesized by a modified vapor diffusion method (Scheme 1). Impressively, the CD-MOF carrier matrix remarkably improves the chemically stable and antioxidant activity of the loaded EGCG in alkaline medium. Meanwhile, the encapsulated EGCG displays a highly therapeutic effect on the tumor cell. Thus, the presently reported CD-MOF-EGCG nanocrystals are more suitable for large-scale applications in industry.

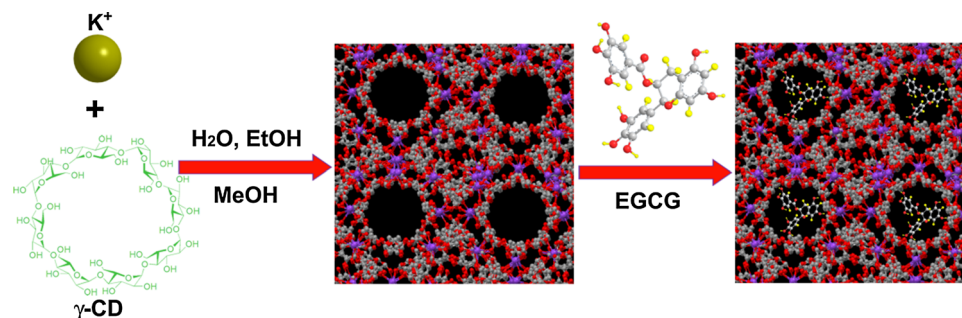
Experimental section

Materials and methods

γ -Cyclodextrin (γ -CD), potassium hydroxide (KOH), and (-)-epigallocatechin gallate (EGCG) were purchased from Sigma-Aldrich. 2,2-diphenyl-1-picrylhydrazyl (DPPH), methanol, and ethanol were purchased from Sinopharm (Shanghai) Chemical Reagent Co., Ltd., China.

The crystalline structure of the samples was measured by the powder X-ray diffraction (PXRD) patterns with Cu target (36 kV, 25 mA) from 3° to 50°. The surface morphology of the samples was monitored by a scanning electron microscopy (SEM, Hitachi S-4800). Fourier transform infrared spectra (FTIR) were recorded on a Nicolette IS 50 FTIR spectrometer. The surface area of the samples was determined by using nitrogen adsorption–desorption isotherm at 77 K with the Micromeritics TriStar II 3020 adsorption analyzer. UV–Vis absorption spectra were investigated by a Shimadzu UV-1800 spectrophotometer. The cytotoxicity of samples was measured through cell viability tests by undifferentiated C6 cells.

Scheme 1 Schematic representation of synthesis and application of CD-MOF for EGCG loading.



Synthesis of CD-MOF

0.324 g of γ -CD and 0.112 g of KOH were firstly dissolved in 20 mL deionized water at room temperature. After dissolved thoroughly, the mixed solution was filtered, and 5 mL of ethanol as an emulsifier was added. Then the solution was sealed in a beaker containing 5 mL of methanol to allow for vapor diffuse into the aqueous solution at 50 °C. After 6 h, the supernatant was transferred into a clean glass tube, and another 10 mL of methanol was added dropwise into the obtained suspension. The mixture was incubated at room temperature for 1 h. The obtained products were collected by centrifugation, washed with methanol three times, and dried under vacuum for 12 h at 45 °C.

Encapsulation of EGCG in CD-MOF

Fifty milligrams of EGCG was firstly dissolved in 10 mL of ethanol, and then the dehydrated CD-MOF (100 mg) was added. After stirring for 36 h at room temperature, the EGCG-loaded CD-MOF was collected by filtration, and washed rapidly with ethanol (5 mL \times 3) to remove EGCG adsorbed on the outer surface of the CD-MOF. The sample was dried at the room temperature. All filtrates were collected and analyzed by UV–Vis spectroscopy and the high-performance liquid chromatography (HPLC).

Antioxidant activity of EGCG-loaded CD-MOF

Antioxidant activity of the samples was evaluated by the DPPH method for testing and comparing the efficiency of the free and encapsulated EGCG with different dose. Briefly, the effects of CD-MOF-EGCG dose were carried out by exposing 1–4 mg of CD-MOF-EGCG to 4 mL of methanol. Then 36 mL of 0.2 mM of DPPH radical solution in methanol was

added. The mixture was shaken in a vortex and allowed to stand in the dark for 30 min at room temperature. The absorbance was measured by a UV–Vis spectrophotometer at the wavelength of 517 nm. The antioxidant activity was expressed as DPPH radical-scavenging activity (RSA) according to the following equation:

$$RSA(\%) = (1 - A_s/A_0) \times 100 \quad (1)$$

where A_s and A_0 are the absorbance at 517 nm of sample and blank DPPH solution, respectively.

Effect of CD-MOF encapsulation on the stability of EGCG in alkaline solution

The DPPH method was also used to evaluate the ability of the CD-MOF to protect EGCG from degradation in alkaline environment. The antioxidant activity of encapsulated and free EGCG was analyzed after dissolution in buffer solution (pH = 10). Four milligrams of the CD-MOF-EGCG (0.8 mg of free EGCG) was added to 10 mL of the pH 10 solution. After specific time intervals, 0.4 mL of the solution was added to 3.6 mL of 0.2 mM of DPPH radical solution. The mixture was shaken in a vortex and allowed to stand in the dark for 30 min, and then the antioxidant activity percentage was measured by a UV–Vis spectrophotometer.

Cytotoxicity assays

The cytotoxic activity of CD-MOF, CD-MOF-EGCG, and free EGCG was evaluated on C6 cells using the MTT (3-(4,5-dimethyl-2-thiazolyl)-2-5-diphenyl-2H-tetrazolium bromide) method. C6 cells (rat glioma cells) were incubated for 24 h with 5% CO_2 at 37 °C prior to the assay in 96-well plates at a density of 1×10^4 cells per well. Subsequently, different concentrations of CD-MOF, CD-MOF-EGCG, and free

EGCG (0, 1, 3, 5, 15, 30, 60, 125, and 250 $\mu\text{g mL}^{-1}$) were added to the medium and incubated for another 24 h. Then, 20 μL of MTT (50 mg mL^{-1}) was added to the cell culture medium and incubated for 4 h. Finally, the medium was replaced by 150 μL of DMSO. The absorbance at 490 nm was monitored by a microplate reader. Non-treated cells were used as a control, and the cell viability was calculated as a percentage of the absorbance of the sample well to that of the cell control. All the experiments were performed in triplicate.

Results and discussion

Adsorption kinetics for EGCG

In order to test the influence of time on the adsorption ability of EGCG onto the CD-MOF, 5 mg of the as-synthesized CD-MOF was suspended in 10 mL of 100 mg L^{-1} EGCG ethanol solution. The amount of the remaining EGCG in the supernatant was determined by UV–Vis absorption spectroscopy. In the presence of CD-MOF nanocrystals, as shown in Fig. 1a, the absorption intensity at 276 nm of EGCG in the solution decreased continuously with the adsorption time. For comparison, the same experiment for free EGCG without adding of CD-MOF was also carried out (Fig. 1b). As can be seen in Fig. 1b, in the absence of CD-MOF, the absorbance remained almost unchanged even over a period of 36 h, suggesting that there is no degradation of EGCG in ethanol under the current adsorption conditions. These findings indicate that decrease in the amount of EGCG in the ethanol with the presence of CD-MOF due to encapsulation into the pores of CD-MOF. The encapsulation rate of EGCG into CD-MOF was determined by first-order kinetics (Fig. 1c). The value of the encapsulation half-life was estimated to be 6.59 h, suggesting that encapsulation of EGCG into the CD-MOF to be a relatively slow process under this adsorption condition. For a higher EGCG loading level, 100 mg of the CD-MOF was added to 10 mL of 5000 mg L^{-1} EGCG ethanol solution. The amount of the EGCG laden in CD-MOF was obtained according to the standard equation. The calibration curve of EGCG was determined by taking absorbance versus EGCG concentration in a range of 0–100 mg L^{-1} as parameters (Fig. 1d). The EGCG content was determined to be 0.26 g of EGCG per gram of the sample.

Characterization of samples

The synthesis of monodispersed and nanosized crystalline MOFs is an important factor for their application in biomedicine. The morphology and size distribution of the as-synthesized CD-MOF crystals were characterized by SEM technique. As shown in Fig. 2, these crystals displayed cubic morphologies with smooth surfaces and uniform size distributions. The representative SEM images reveal that the size of the CD-MOF particles is around 500 nm. Although the literature reported that CD-MOFs carriers exhibit high drug loading capacity, the size of them is quite big. And we all know that downsizing materials to the nanoscale is a suitable method to tackle down new application in biomedicine. Owing to their smaller particle size, nanomaterials can improve the drug delivery for the treatment of diseases. In this work, the particle size of the as-synthesized CD-MOF is much smaller than that of the reported in the literature [29, 31–33].

The corresponding crystallographic structures of the as-synthesized CD-MOF before and after EGCG loaded were characterized by PXRD and IR analysis. As shown in Fig. 3, the PXRD pattern of pure CD-MOF confirmed the crystalline morphologies of the sample, which is consistent with reported in the literature [29]. At the same time, the PXRD pattern shown in Fig. 3 reveals that EGCG loading does not influence the crystallinity of the CD-MOF crystals. EGCG is a crystalline green tea catechin with characteristic PXRD peaks quite different from those of CD-MOF. However, there are no PXRD peaks belonging to those of EGCG observed in the EGCG-loaded CD-MOF sample, which can be ascribed to that EGCG is entrapped in a molecular state in the porous of CD-MOF.

The FTIR spectra of the free EGCG and CD-MOF with and without loaded EGCG are presented in Fig. 4. The FTIR spectra of the CD-MOF nanocrystals showed the band located at around 3287 cm^{-1} can be ascribed to the –OH group of the γ -CD. In the spectra of EGCG-loaded CD-MOF sample, the band of –OH group is shifted to the higher values (3310 cm^{-1}) compared with the pure CD-MOF. The upward shift of the –OH stretching vibration suggesting that the EGCG can be encapsulated onto the CD-MOF via the interaction between the –OH group of CD-MOF and EGCG. Furthermore, the prominent bands around 3359 and 3483 cm^{-1} for the characteristics of phenolic

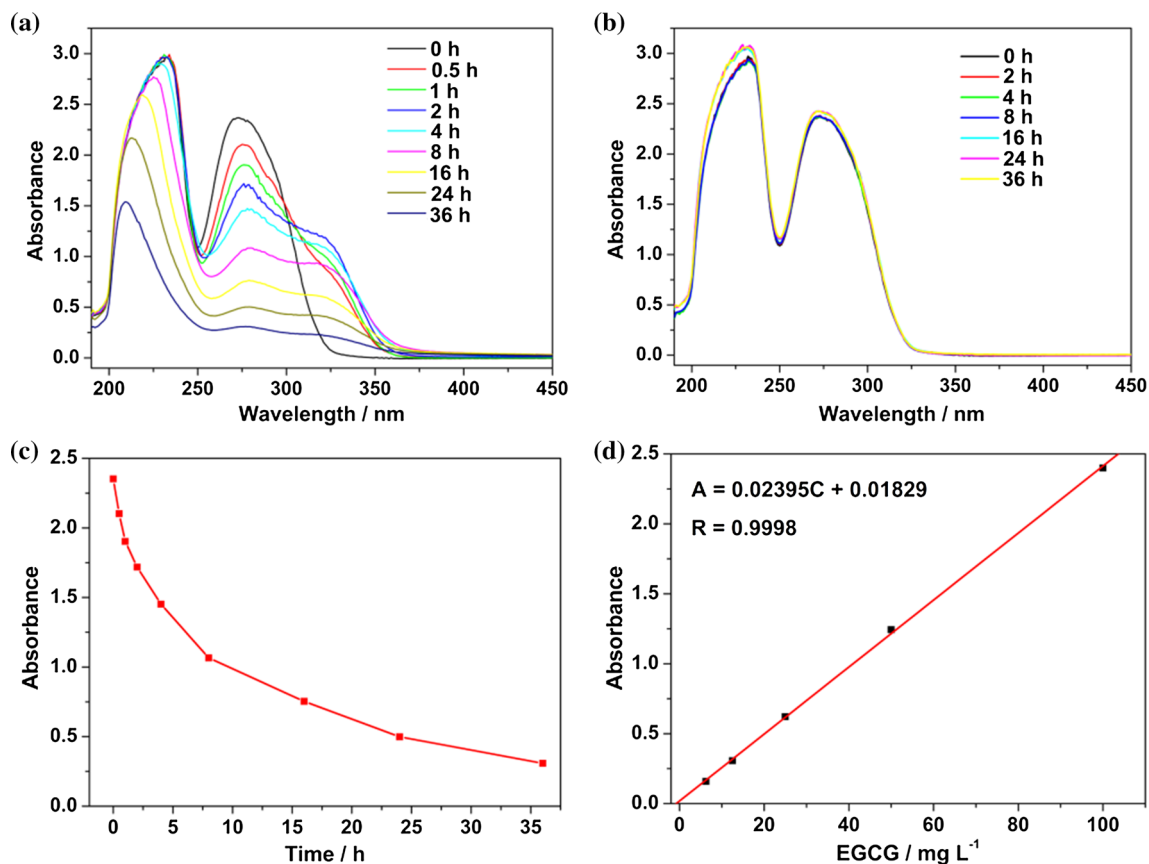
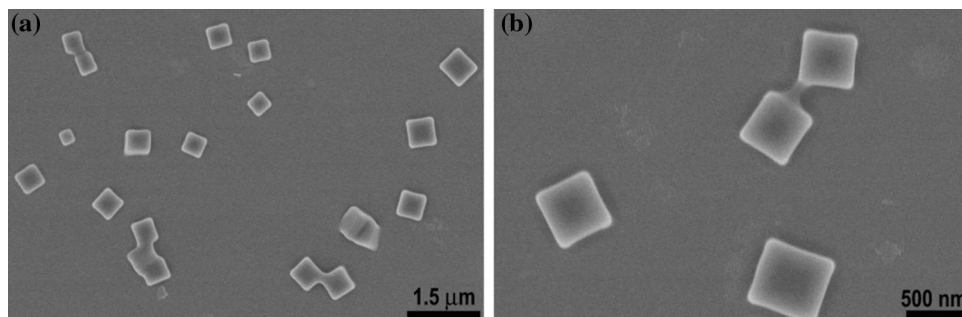


Figure 1 UV–Vis absorption spectra of EGCG in the presence (a) and absence (b) of CD-MOF in ethanol with time. c Variation of absorbance at 276 nm of EGCG in the presence of CD-MOF and d the calibration curve of EGCG in ethanol.

Figure 2 SEM images of the as-synthesized CD-MOF (a, b).



hydroxyl vibration of EGCG were not present in the spectra of CD-MOF-EGCG, indicating a hydrogen bond type interaction between the phenolic hydroxyl group of EGCG and the $-OH$ group of the γ -CD of CD-MOF framework.

The porous features of the CD-MOF before and after encapsulation of EGCG were investigated by the nitrogen adsorption–desorption isotherms (Fig. 5). The Brunauer–Emmett–Teller (BET) surface area and pore volume of the obtained CD-MOF were calculated to be $175 \text{ m}^2 \text{ g}^{-1}$ and $0.11 \text{ cm}^3 \text{ g}^{-1}$, respectively.

The adsorption of EGCG results in a dramatic decrease in both BET surface area and pore volume of the CD-MOF nanocrystals (Fig. 5a). After the catechin encapsulation, the BET surface area and pore volume of the nanocrystals decreased to $45 \text{ m}^2 \text{ g}^{-1}$ and $0.03 \text{ cm}^3 \text{ g}^{-1}$, respectively, which implies that the EGCG occupies almost all pore space in the frameworks. Moreover, estimation of the pore size distribution by Barrett–Joyner–Halenda (BJH) method shows three pore sizes at 1.01, 1.21, and 1.45 nm for the as-synthesized CD-MOF nanocrystals (Fig. 5b),

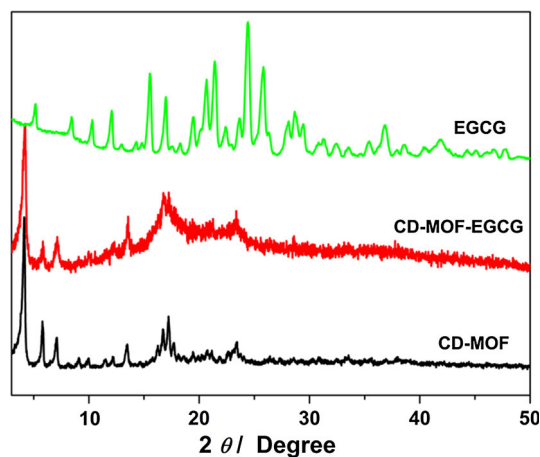


Figure 3 PXRD patterns for EGCG, CD-MOF and the EGCG-loaded CD-MOF (CD-MOF-EGCG).

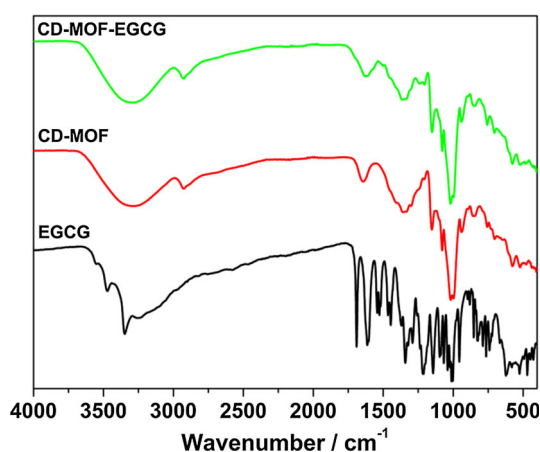


Figure 4 FTIR spectra of EGCG, CD-MOF and the EGCG-loaded CD-MOF (CD-MOF-EGCG).

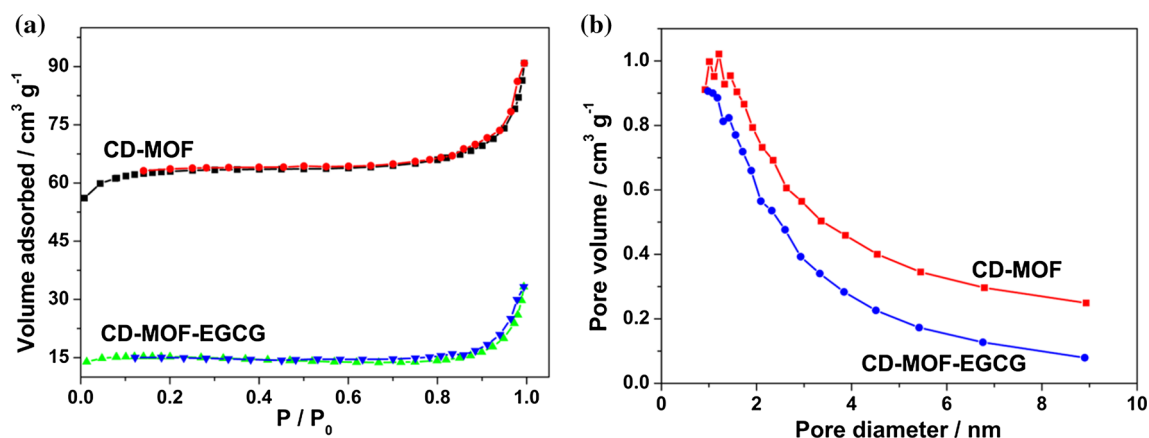


Figure 5 Nitrogen adsorption–desorption isotherms (a) and the corresponding pore size distribution analysis obtained using BJH method (b) of CD-MOF and the EGCG-loaded CD-MOF (CD-MOF-EGCG).

attributed to micropore cage, which is similar with the previously reported for CD-MOF [32]. In the meantime, the pore volume of the pores was significantly reduced after the EGCG incorporation. All these results upon EGCG encapsulation supported that EGCG was successfully trapped within CD-MOF nanocrystals.

Antioxidant activity of EGCG-loaded CD-MOF

We have chosen CD-MOF to encapsulate catechin due to its nontoxic and biocompatibility. To explore the potential application of nanosize CD-MOF as catechin vehicles, antioxidant and anticancer catechin EGCG, as a typical example, was trapped within CD-MOF. The radical-scavenging activity (RSA) of both free and encapsulated EGCG was evaluated by the model DPPH decolorization assay to ascertain whether the encapsulation process had an impact on the antioxidant activity of the catechin molecular and the results are presented in Fig. 6. It was shown that there was no antioxidant activity of the unloaded CD-MOF, thus, the antioxidant activity of the MOF was neglected. Therefore, the RSA of the CD-MOF-EGCG was attributed only to the contribution of the loaded EGCG. From Fig. 6, we can see that the final antioxidant activity increased with the amount of CD-MOF-EGCG addition (Fig. 6). As the amount of CD-MOF-EGCG increased from 1 to 4 mg, the antioxidant activity gradually increased from 12 to 50%. While no significant differences were found between the antioxidant activity of the 4 mg of CD-MOF-EGCG (50%), corresponding to 0.8 mg of EGCG, and the

same amount of free EGCG (55%), indicating that the RSA of the encapsulated EGCG was almost retained during the encapsulation process.

Stabilization of EGCG in the loaded CD-MOF

Further, we investigated the stability of EGCG in the CD-MOF structure. We all know that EGCG is relatively stable in organic solvents like ethanol, but it is quite unstable in the alkaline solution [34]. The EGCG-loaded CD-MOF described in this work is designed to overcome this problem. It is worth to mention that the dissociation of the EGCG-loaded CD-MOF framework in water leads to the formation of a water-soluble complex that involves EGCG, CD, and potassium cations. Protection ability of CD-MOF for the loaded EGCG was also tested by the DPPH method. Figure 7 shows comparison of the antioxidant activity performance of the dissolved EGCG without and with the protection of CD-MOF in water under alkaline conditions (pH = 10) in five consecutive days, respectively. At the beginning, the free EGCG shows a little higher activity due to the diffusion of DPPH molecular into the EGCG is easy. However, the antioxidant activity of free EGCG drops rapidly in the subsequent days. As can be seen from Fig. 7, the antioxidant activity of the free EGCG decreases significantly from 55 to 11% after 5 days. In contrast, the EGCG protected by CD-MOF maintain its activity well in the 5 days. The antioxidant activity of CD-MOF-EGCG only drops by 8% after 5 days. These results suggest that the encapsulation of EGCG

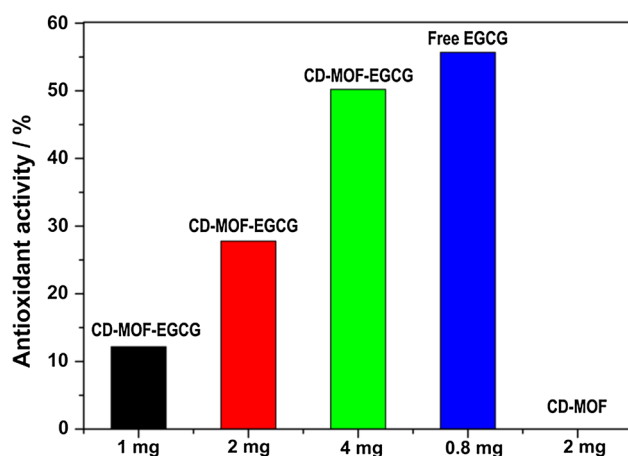


Figure 6 Antioxidant activity of free and encapsulated EGCG, together with pure CD-MOF blank.

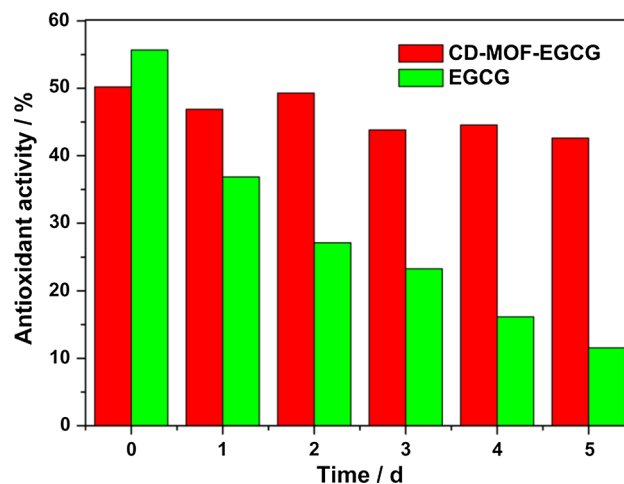


Figure 7 Time-dependent radical scavenging activity of EGCG-loaded CD-MOF and free EGCG in pH 10.

in the pores of CD-MOF could effectively protect EGCG from the degradation in alkaline solutions. Under alkaline conditions, the phenolic hydroxyl group of EGCG becomes de-protonated, and it is likely to undergo degradation by undergoing oxidation to a semiquinone radical intermediate and form quinone oxidized products. In contrast, for CD-MOF-EGCG, the EGCG can be adsorbed onto the porous via the interactions between the hydroxyl group of EGCG and the -OH group of the organic part of the framework, thus enhancing the chemical stability and antioxidant activity. Therefore, in the presence of this CD-MOF-EGCG system, the stability of EGCG was substantially enhanced due to incorporation within the pores of the CD-MOF.

Cytotoxicity

In vitro cell viabilities of CD-MOF, CD-MOF-EGCG, and free EGCG on C6 cells are evaluated by MTT assay to study the toxicity of CD-MOF and the therapeutic effect of CD-MOF-EGCG (Fig. 8). As shown in Fig. 8, after an incubation time of 24 h with C6 cells, the C6 cells treated with the CD-MOF without loading EGCG exhibited a high cell viability (> 95%) when the concentrations of the CD-MOF ranged at 0–250 $\mu\text{g mL}^{-1}$, indicating that the as-synthesized CD-MOF nanocrystals were safe, biocompatible, and nontoxic. However, after loading with EGCG, the CD-MOF-EGCG nanocrystals show a stronger cell growth inhibition effect on C6 cells compared to the presence of CD-MOF. The C6 cell viability value decreased to 44% when the concentration of the CD-

MOF-EGCG is only $250 \mu\text{g mL}^{-1}$. For free EGCG, as expected, a relatively lower cell viability value (33%) is observed at the concentration of $250 \mu\text{g mL}^{-1}$. At first glance, one may argue that the cytotoxicity of CD-MOF-EGCG is reduced against C6 cells compared to the cytotoxicity of EGCG alone, so that the cytotoxicity of the CD-MOF-EGCG maybe entirely attributed to the presence of EGCG. However, this cell viability value was measured based on the same total particles concentration, namely $250 \mu\text{g mL}^{-1}$ (Fig. 8). The actual content of EGCG in the CD-MOF-EGCG nanocrystals is only $51.58 \mu\text{g mL}^{-1}$, corresponding to only 20.63% of pure EGCG used. If we scale up to the same amount of EGCG used, the cell viability value will be significantly lower after the EGCG is loaded with porous CD-MOF. Therefore, these results clearly demonstrate that CD-MOF plays an important role in the enhancement of induced cell death activity of the CD-MOF-EGCG nanocrystals, which suggests that the CD-MOF-EGCG can be potentially applied for cancer treatment.

Conclusions

In conclusion, this work demonstrates a promising catechins encapsulation system based on nanoscale CD-MOF for antioxidant activity and tumor therapy. The nontoxic and biocompatible CD-MOF nanocarriers have been fabricated by using a simple modified vapor diffusion method. For the first time, the as-synthesized CD-MOF used as a novel carrier for the

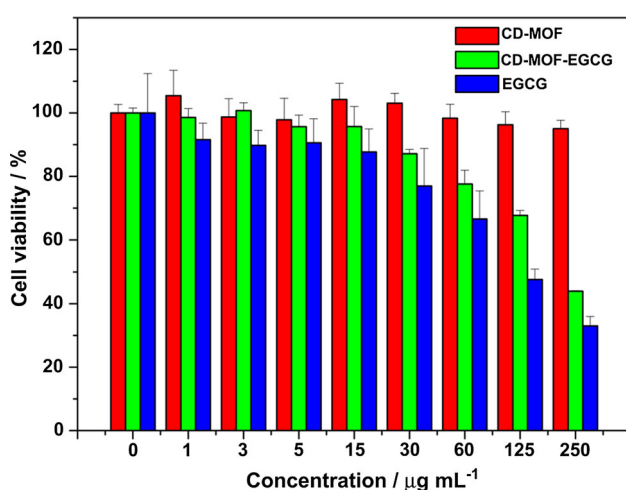


Figure 8 In vitro cell viabilities of C6 cells against the CD-MOF with and without EGCG loading at various concentrations.

encapsulation of EGCG through a hydrogen bond type interaction between the phenolic hydroxyl group of EGCG and the $-\text{OH}$ group of the organic part of CD-MOF. Significantly, the antioxidant activity results of CD-MOF-EGCG shows excellent chemical stability of EGCG in alkaline solutions. The cytotoxicity results demonstrate that the obtained CD-MOF nanocrystals were safe and nontoxic. Moreover, encapsulation of EGCG in the pores of CD-MOF shows an outstanding efficacy in killing the cancer cells. These findings demonstrate the significant potential of scale-up synthesis of nanoscale CD-MOF and exploration of their properties to store and stabilize catechins for biomedical applications.

Acknowledgements

This work was supported by the National Natural Science Foundation of China (NSFC, 21501003), Natural Science Foundation of Anhui Province (1608085QB27), China Postdoctoral Science Foundation funded project (2015M581973), the Scientific Research Foundation of Anhui Agricultural University (GrantNo. yj2015-26), and Provincial Undergraduate Training Programs for Innovation and Entrepreneurship of Anhui Agriculture University(201710364054).

References

- [1] Grzesik M, Bartosz G, Dziedzic A, Narog D, Namiesnik J, Sadowska-Bartosz I (2018) Antioxidant properties of ferrous flavanol mixtures. *Food Chem* 268:567–576
- [2] Iñiguez-Franco F, Soto-Valdez H, Peralta E, Fernando Ayala-Zavala J, Auras R, Gámez-Meza N (2012) Antioxidant activity and diffusion of catechin and epicatechin from antioxidant active films made of poly (L-lactic acid). *J Agric Food Chem* 60:6515–6523
- [3] Aree T, Jongrungruangchok S (2016) Enhancement of antioxidant activity of green tea epicatechins in β -cyclodextrin cavity: single-crystal X-ray analysis, DFT calculation and DPPH assay. *Carbohydr Polym* 151:1139–1151
- [4] Bae KH, Tan S, Yamashita A, Ang WX, Gao SJ, Wang S, Chung JE, Kurisawa M (2017) Hyaluronic acid-green tea catechin micellar nanocomplexes: fail-safe cisplatin nanomedicine for the treatment of ovarian cancer without off-target toxicity. *Biomaterials* 148:41–53

- [5] Ray L, Kumar P, Gupta KC (2013) The activity against Ehrlich's ascites tumors of doxorubicin contained in self assembled, cell receptor targeted nanoparticle with simultaneous oral delivery of the green tea polyphenol epigallocatechin-3-gallate. *Biomaterials* 34:3064–3076
- [6] Dube A, Ng K, Nicolazzo JA, Larson I (2010) Effective use of reducing agents and nanoparticle encapsulation in stabilizing catechins in alkaline solution. *Food Chem* 122:662–667
- [7] Chanphai P, Tajmir-Riahi HA (2018) Conjugation of tea catechins with chitosan nanoparticles. *Food Hydrocoll* 84:561–570
- [8] Ahmad M, Mudgil P, Gani A, Hamed F, Masoodi FA, Maqsood S (2019) Nano-encapsulation of catechin in starch nanoparticles: characterization, release behavior and bioactivity retention during simulated in vitro digestion. *Food Chem* 270:95–104
- [9] Gómez-Mascaraque LG, Soler C, Lopez-Rubio A (2016) Stability and bioaccessibility of EGCG within edible microhydrogels. Chitosan vs. gelatin, a comparative study. *Food Hydrocoll* 61:128–138
- [10] Aree T, Jongrungruangchok S (2018) β -Cyclodextrin encapsulation elevates antioxidant capacity of tea: a closing chapter on non-epicatechins, atomistic insights from X-ray analysis, DFT calculation and DPPH assay. *Carbohydr Polym* 194:24–33
- [11] Kirchon A, Feng L, Drake HF, Joseph EA, Zhou H-C (2018) From fundamentals to applications: a toolbox for robust and multifunctional MOF materials. *Chem Soc Rev* 47:8611–8638
- [12] Zhou H-C, Long JR, Yaghi OM (2012) Introduction to metal-organic frameworks. *Chem Rev* 112:673–674
- [13] Jiao L, Wang Y, Jiang H-L, Xu Q (2018) Metal-organic frameworks as platforms for catalytic applications. *Adv Mater* 30:1703663
- [14] Li G, Zhao S, Zhang Y, Tang Z (2018) Metal-organic frameworks encapsulating active nanoparticles as emerging composites for catalysis: recent progress and perspectives. *Adv Mater* 30:1800702
- [15] Wu L, Tong Y, Gu L, Xue Z, Yuan Y (2018) MOFs as an electron-transfer-bridge between a dye photosensitizer and a low cost Ni₂P co-catalyst for increased photocatalytic H₂ generation. *Sustain Energy Fuels* 2:2502–2506
- [16] Liu X-L, Wang R, Zhang M-Y, Yuan Y-P, Xue C (2015) Dye-sensitized MIL-101 metal organic frameworks loaded with Ni/NiOx nanoparticles for efficient visible-light-driven hydrogen generation. *APL Mater* 3:104403
- [17] Wang R, Gu L, Zhou J, Liu X, Teng F, Li C, Shen Y, Yuan Y (2015) Quasi-polymeric metal-organic framework UiO-66/g-C₃N₄ heterojunctions for enhanced photocatalytic hydrogen evolution under visible light irradiation. *Adv Mater Interfaces* 2:1500037
- [18] Yuan Y-P, Yin L-S, Cao S-W, Xu G-S, Li C-H, Xue C (2015) Improving photocatalytic hydrogen production of metal-organic framework UiO-66 octahedrons by dye-sensitization. *Appl Catal B Environ* 168–169:572–576
- [19] Simon-Yarza T, Mielcarek A, Couvreur P, Serre C (2018) Nanoparticles of metal-organic frameworks: on the road to in vivo efficacy in biomedicine. *Adv Mater* 30:1707365
- [20] Horcajada P, Chalati T, Serre C et al (2010) Porous metal-organic-framework nanoscale carriers as a potential platform for drug delivery and imaging. *Nat Mater* 9:172–178
- [21] Yang Y, Xia F, Yang Y, Gong B, Xie A, Shen Y, Zhu M (2017) Litchi-like Fe₃O₄@Fe-MOF capped with HAp gatekeepers for pH-triggered drug release and anticancer effect. *J Mater Chem B* 5:8600–8606
- [22] Bunzen H, Kolbe F, Kalytta-Mewes A, Sastre G, Brunner E, Volkmer D (2018) Achieving large volumetric gas storage capacity in metal-organic frameworks by kinetic trapping: a case study of Xenon loading in MFU-4. *J Am Chem Soc* 140:10191–10197
- [23] Zhang X, Zhang Q, Yue D et al (2018) Flexible metal-organic framework-based mixed-matrix membranes: a new platform for H₂S sensors. *Small* 14:1801563
- [24] Ke F, Jiang J, Li Y, Liang J, Wan X, Ko S (2017) Highly selective removal of Hg²⁺ and Pb²⁺ by thiol-functionalized Fe₃O₄@metal-organic framework core-shell magnetic microspheres. *Appl Surf Sci* 413:266–274
- [25] Ke F, Peng C, Zhang T, Zhang M, Zhou C, Cai H, Zhu J, Wan X (2018) Fumarate-based metal-organic frameworks as a new platform for highly selective removal of fluoride from brick tea. *Sci Rep* 8:939
- [26] Horcajada P, Gref R, Baati T et al (2012) Metal-organic frameworks in biomedicine. *Chem Rev* 112:1232–1268
- [27] Qiu C, Wang J, Qin Y, Fan H, Xu X, Jin Z (2018) Green synthesis of cyclodextrin-based metal-organic frameworks through the seed-mediated method for the encapsulation of hydrophobic molecules. *J Agric Food Chem* 66:4244–4250
- [28] Forgan RS, Smaldone RA, Gassensmith JJ et al (2012) Nanoporous carbohydrate metal-organic frameworks. *J Am Chem Soc* 134:406–417
- [29] Smaldone RA, Forgan RS, Furukawa H, Gassensmith JJ, Slawin AMZ, Yaghi OM, Stoddart JF (2010) Metal-organic frameworks from edible natural products. *Angew Chem Int Ed* 49:8630–8634
- [30] Li H, Lv N, Li X et al (2017) Composite CD-MOF nanocrystals-containing microspheres for sustained drug delivery. *Nanoscale* 9:7454–7463
- [31] Hartlieb KJ, Ferris DP, Holcroft JM, Kandela I, Stern CL, Nassar MS, Botros YY, Stoddart JF (2017) Encapsulation of

- ibuprofen in CD-MOF and related bioavailability studies. *Mol Pharm* 14:1831–1839
- [32] Li H, Hill MR, Huang R, Doblin C, Lim S, Hill AJ, Babarao R, Falcaro P (2016) Facile stabilization of cyclodextrin metal-organic frameworks under aqueous conditions via the incorporation of C-60 in their matrices. *Chem Commun* 52:5973–5976
- [33] Moussa Z, Hmadeh M, Abiad MG, Dib OH, Patra D (2016) Encapsulation of curcumin in cyclodextrin-metal organic frameworks: dissociation of loaded CD-MOFs enhances stability of curcumin. *Food Chem* 212:485–494
- [34] Wang Q, Cao J, Yu H, Zhang J, Yuan Y, Shen X, Li C (2019) The effects of EGCG on the mechanical, bioactivities, cross-linking and release properties of gelatin film. *Food Chem* 271:204–210

Publisher's Note Springer Nature remains neutral with regard to jurisdictional claims in published maps and institutional affiliations.